GEOSCIENCES

journal homepage: www.gsjournal.ir

Geologic and geochemical investigation on the Mn veins in Jonub-E Sehchangi, SW Birjand, Southern Khorasan province (east Iran)

Behnaz Barghi[1*], Ali Asghar Calagari[2], Mohammad Hossein Zarrinkoub[3] and Vartan Simmonds[4]

[1]*Ph.D., Department of Earth Sciences, Faculty of Natural Sciences, University of Tabriz, Tabriz, Iran*

[2]*Professor, Department of Earth Sciences, Faculty of Natural Sciences, University of Tabriz, Tabriz, Iran*

[3]*Professor, Department of Geology, University of Birjand, Birjand, Iran*

[4]*Associate Professor, Research Institute for Fundamental Sciences, University of Tabriz, Tabriz, Iran*

ARTICLE INFO

Received: 2017 July 23

Accepted: 2017 December 24

Available online: 2018 March 17

Keywords:
Mn vein
Jonub-E Sehchangi
Andesite
Pyrolusite
Psilomelane
Argillic alteration

**Corresponding author:*
B. Barghi
E-mail:barghibehnaz@yahoo.com

ABSTRACT

Mn-bearing veins of Jonub -E Sehchangi are located 200 km southwest of Birjand, Southern Khorasan province (east of Iran). These veins are hosted by andesitic rocks of Eocene to Oligocene ages. Ore minerals identified by XRD method and mineralographic studies and are pyrolusite, cryptomelane, psilomelane, hollandite, hematite and goethite, displaying colloform and open-space filling textures. Gypsum, halite, barite, carbonate and silica are the gangue minerals. Alteration zones, specifically argillic alteration zone, are developed along the vein within the andesitic wall rocks. Based on the mineralogical and geochemical data, the primary manganese minerals were Mn oxides and hydroxides, which have gradually been converted to psilomelane and hollandite, and finally to pyrolusite. The average grade of Mn within the veins is 38.61%. Considering the average Mn/Fe ratio (about 48.55) in the Mn-bearing veins, as well as the positive correlation of Sr, U and Ba with Mn, mineralization in this area show hydrothermal origin.

1- Introduction

Manganese deposits in Iran are temporally and spatially classified into six groups: 1- Mn deposits of late Pre cambrian-early Cambrian, which are volcanic-sedimentary and volcanic in nature, occurred in central Iran and Azarbaidjan (NW Iran) (Monazami Bagherzadeh, 1994); 2- Mn deposits of late Paleozoic, encompassing volcanic-sedimentary Fe-rich Mn deposits of eastern and central Iran and the Sanandaj-Sirjan zone (Bonyadi and Moore, 2006); 3-manganese mineralizations of early Cretaceous in the form of Mn and Mn-Fe deposits in the Sanandaj-Sirjan zone with volcanic-sedimentary origin (Nabatian et al., 2015); 4- Mn mineralization of late Cretaceous-Paleocene, which are related to the ophiolitic complexes (Neyriz, Sabzevar, Birjand and Azarbaidjan ophiolitic ridges) (Taghizadeh et al., 2012); 5- Mn deposits of Eocene-Oligocene ages, which include most of the known Mn deposits of Iran. They have hydrothermal origin and display vast distribution in Iran, especially in central and north of Iran. They are generally found in areas with outcrops of Eocene andesitic-dacitic rocks (Zarasvandi et al., 2013); 6-Mn mineralization in Miocene-Pliocene, which mainly occurred in Azarbaidjan area (NW Iran; Simmonds and Malek Ghasemi, 2007). Mn veins of Jonub-E Sehchangi in SW Birjand (Fig. 1) belong to Eocene-Oligocene age. This contribution aims to investigate on the mineralogy, petrography and geochemistry (element ratios and variations) of the Mn veins in the Jonub-E Sehchangi area in order to elucidate their genesis and the formation mechanism, as well as the distribution of major, minor and trace elements within these veins.

2- Method of investigation

Field studies were conducted in order to recognize the rock units, as well as alteration and mineralization zones.

Sampling of the ores was performed both systematically and irregularly along the six trenches dug perpendicular into the veins. 25 ore and host-rock samples were collected randomly for petrographic and mineralographic studies, of which 20 thin-polished sections were prepared and studied at the economic geology lab, University of Tabriz. Systematic sampling was carried out along the trench #4, where a 1.5 m thick and 3.5 m long Mn vein is cropped out. Seven samples were systematically collected from center towards the wall rock of the vein (Fig. 2b) and analysed for major, minor and trace elements by ICP-ES-MS method at ACME lab (Canada) (Table 1). SiO_2 content was determined by ICP-MS method. Furthermore, seven samples were analysed by XRD method (using Philips 1840 differactometer with CuKα, graphite chromator, 40kV, 30mA, and 2θ angle from 10° to 50° and step size of 0.02) at the University of Birjand (Iran).

3- Regional geology

The study area is located 200 km southwest of Birjand, Southern Khorasan province (east of Iran). The Jonub -E Sehchangi prospecting area is located within the 1:100,000 geologic map of Jonub- E- Sehchangi (Bolourian et al., 2004). According to the classification of the structural zones of Iran, this area lies in the Lut block (Fig. 1). The Lut Block (Eastern Iran) extends over 900 km in the north-south direction and about 200 km in the east-west direction. It is confined by the Nayband fault and Shotori Range at the west and the Sistan suture zone and Nehbandan Fault at the east. The most widespread rock types across the Lut-Sistan region include lavas and pyroclastic rocks, as well as sub-volcanic rocks of Eocene - Oligocene ages (Karimpour et al., 2011). Volcanic rocks are formed during the subduction to post-collisional stages between Arabian and Turan plates (Camp and Griffis, 1982; Tirrul et al., 1983; Berberian et al., 1999), covering a large part of the east of Iran (300×400 km^2; Richards et al., 2012; Pang et al., 2013). These rocks have high potential for various types of mineralization in subduction, collisional and post-collisional settings in the region (Lotfi, 1982; Tarkian et al., 1983; Jung et al., 1983; Saadat et al., 2008 and 2009, Walker et al., 2009; Arjmandzadeh et al., 2011; Arjmandzadeh, and Santos, 2014). Contrary to the volcanic belts of Iran, e.g., Urumieh-Dokhtar and Alborz volcanic-plutonic belts, which have linear or curved trend, volcanics in east of Iran display a scattered pattern. Volcanism in east of Iran is confined to the Sistan suture zone in the east and the Nayband fault in the west (Walker et al., 2009). The study area lies within the volcanic rocks in east of Iran (see Fig. 1).

4- Geology of the study area

The main lithologic units in the study area include hornblende andesites and pyroxene andesites of Eocene-Oligocene age (Karimpour et al., 2011).

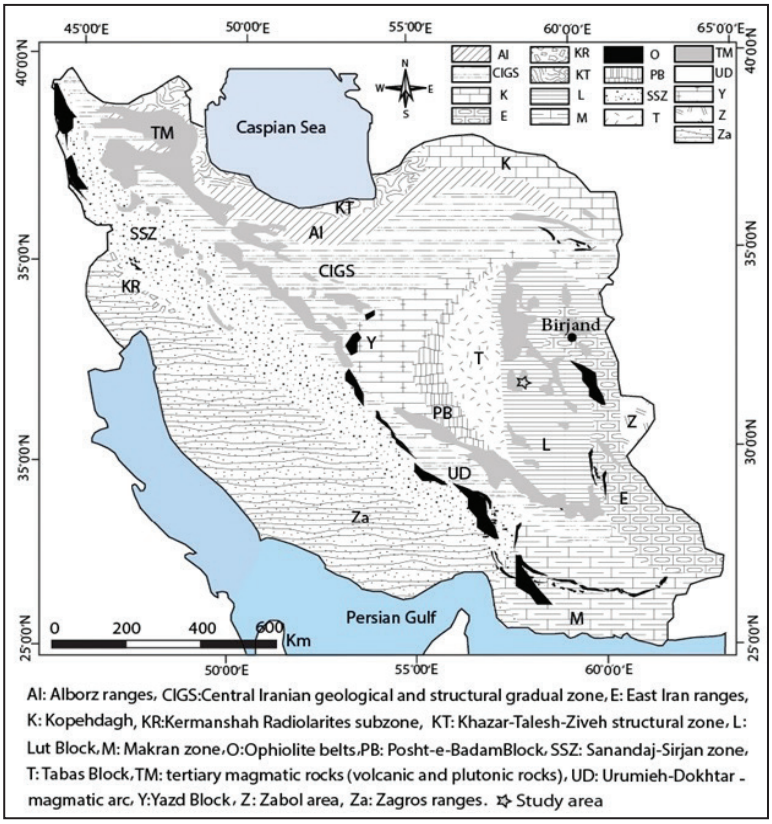

Fig. 1- Simplified structural map of Iran, and the location of volcanic rocks in east of Iran and the study area in the Lut block (Aghanabati, 1998).

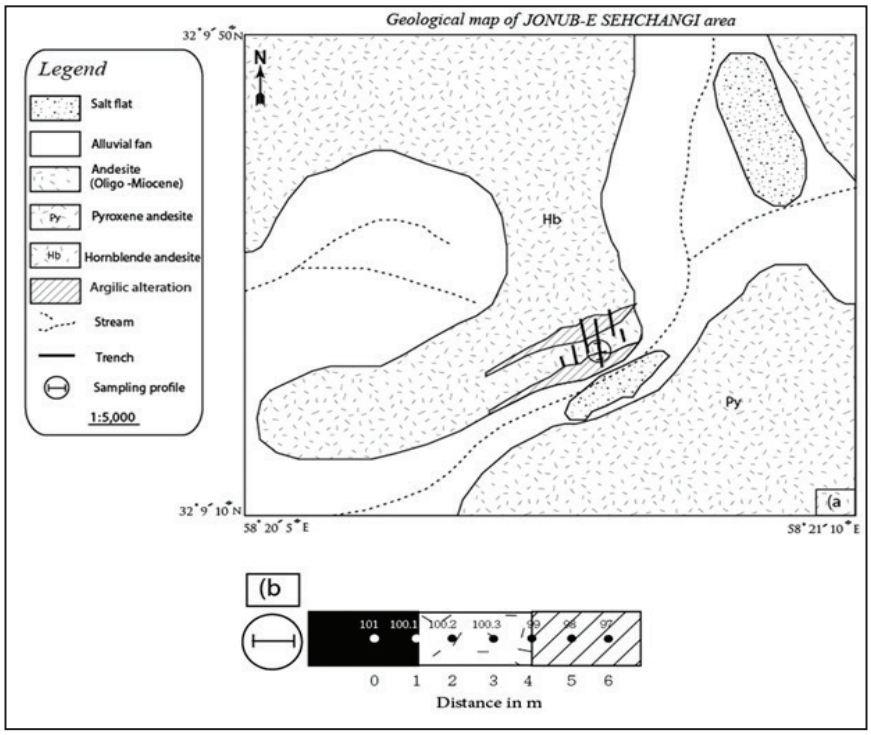

Fig. 2- a) Geologic map of the study area (1:5000); b) a cross-section across which the samples were collected (from the center of the vein toward the wall rocks).

Mn veins are hosted by Eocene-Oligocene purple-colored hornblende andesites (Fig. 3 a and b). The host rock suffered argillic alteration in both sides of the Mn vein, which is observed along the long trench (Fig. 3c). Furthermore, a 20-30 cm thick halite lens is found at the upper part of the trenches (Fig. 3d).

5- Petrography of the host volcanic rocks

The host rock of the Mn veins is hornblende andesite of Eocene - Oligocene ages (Fig. 2a). Andesitic rocks are purple in color, with distinct white plagioclase phenocrysts in hand specimens, which are euhedral to subhedral under the microscope, occurring as both phenocrysts and microlite and comprise about 60% of the rock. It ranges in composition from andesine to labradorite. It was altered to clay and carbonate minerals, accompanied by lesser amounts of epidote. Aggregates of plagioclase phenocrysts form glomero-porphyritic texture. Background is mainly made of plagioclase microlites. Hornblende (about 30%) is the main ferro-magnesian mineral, with prismatic and sometimes hexahedral habit and shows oxidized rims. Biotite (about 10%) is the second ferro-magnesian mineral in order of abundance. The biotite books are euhedral to subhedral, sometimes being altered to opaque minerals and show oxidized margins. Clinopyroxene is rarely found within the host andesites (Fig. 4a). Additionally, carbonate and silicic veinlets and zeolite (chabasite) are also found under the microscope (Fig. 4b).

6- Mineralography

Due to the difficulty in identifying the Mn minerals under the microscope, ore samples were analysed by XRD method according to which, the main ore minerals of the veins are pyrolusite, psilomelane, cryptomelane and hollandite, accompanied lesser amounts of hematite, goethite and chalcopyrite. Pyrolusite is the most abundant Mn phase. Mn vein displays colloform and open-space filling textures (Fig. 4c and d). Goethite also depicts colloform texture (Fig. 4c). Meanwhile, open-space fillings of pyrolusite and silica are found within the carbonates (Fig. 4d).

7- Geochemistry

In order to study the ore chemistry, seven samples were systematically collected along the trench #4 from the center of manganese vein towards the wall rocks (Fig. 2b). ICP-ES-MS data are provided in the Table 1 based on which, we have tried to determine the probable source of metal and the ore-formation setting.

7- 1. Mn/Fe ratio

Mn and Fe are differentiated on the basis of their solubilities, during precipitation from hydrothermal fluid. Mn/Fe ratios less than 1 testify to Mn deposition in lake environments, while ratios about 1 indicate a hydrogenous origin. Ratios between <0.1 and >10 are characteristic of hydrothermal deposits (Nicholson, 1992).

Table 1- ICP-ES-MS analysis data of the major, minor and trace elements in samples taken from the Jonub-e-Sehchangi Mn deposit.

Method MA270	Unit MDL	101	100.1	100.2	100.3	99	98	97
Mo	0.5ppm	26.2	15.9	15.4	22.3	18.8	23.6	12.0
Cu	0.5ppm	353.0	289.7	287.8	276.7	288.9	858.7	1999.9
Pb	0.5ppm	190.9	127.6	144.6	110.2	126.8	244.0	856.6
Zn	5ppm	614	353	347	433	505	869	1489
Ag	0.5ppm	<0.5	<0.5	<0.5	<0.5	<0.5	<0.5	<0.5
Ni	0.5ppm	44.4	28.0	31.8	38.2	38.4	42.7	39.1
Co	1ppm	24	13	15	15	16	43	61
Mn	5ppm	408239	364076	358539	330227	285647	157879	62936
Fe	0.01%	0.36	0.41	0.53	0.86	1.24	2.56	2.54
As	5ppm	13871	11286	8937	7642	14269	32371	45133
U	0.5ppm	7.4	3.5	3.3	3.3	5.9	3.1	3.7
Th	0.5ppm	0.6	0.5	0.8	1.1	2.1	4.4	4.9
Sr	5ppm	2430	2284	1999	744	1681	1670	1990
Cd	0.5ppm	<0.5	<0.5	<0.5	<0.5	<0.5	<0.5	<0.5
Sb	0.5ppm	788.8	694.2	675.0	599.9	719.2	327.6	262.2
Bi	0.5ppm	<0.5	<0.5	<0.5	<0.5	<0.5	<0.5	<0.5
V	10ppm	226	100	99	97	147	271	183
Ca	0.01%	4.87	6.13	5.46	9.77	8.52	4.23	10.46
P	0.01%	0.02	0.02	0.02	0.02	0.03	0.05	0.04
La	0.5ppm	4.6	4.9	5.9	5.7	7.2	10.5	12.9
Cr	1ppm	17	19	20	24	20	36	27
Mg	0.01%	0.47	0.36	0.44	0.56	0.49	0.26	0.67
Ba	5ppm	20040	6853	7652	7915	12797	8503	8650
Ti	0.01%	0.031	0.031	0.041	0.048	0.094	0.219	0.192
Al	0.01%	0.75	0.69	0.86	1.08	1.96	4.34	4.52
Na	0.01%	0.33	0.23	0.31	0.30	0.20	0.47	0.80
K	0.01%	0.89	0.53	0.72	0.47	2.40	2.98	2.54
W	0.5ppm	324.5	178.5	210.9	179.8	208.6	155.5	59.9
Zr	0.5ppm	6.9	6.5	7.7	11.3	16.1	40.4	37.3
Ce	5ppm	6	<5	6	8	11	19	23
Sn	0.5ppm	<0.5	<0.5	<0.5	<0.5	<0.5	0.7	0.6
Y	0.5ppm	6.1	6.6	5.8	6.8	8.3	11.5	12.7
Nb	0.5ppm	<0.5	<0.5	0.6	0.9	1.5	3.5	2.9
Ta	0.5ppm	<0.5	<0.5	<0.5	<0.5	<0.5	<0.5	<0.5
Be	5ppm	10	11	11	10	9	<5	6
Sc	1ppm	2	2	3	5	3	9	12
Li	0.5ppm	16.1	14.6	26.2	26.5	22.2	67.3	31.0
S	0.05%	0.10	0.24	0.23	0.21	0.15	<0.05	0.06
Rb	0.5ppm	35.6	24.1	33.4	22.3	107.4	109.6	110.2
Hf	0.5ppm	<0.5	<0.5	<0.5	<0.5	0.6	1.3	1.0
Se	5ppm	<5	<5	<5	<5	<5	<5	<5
Method LF300	Unitn MDL	101	100.1	100.2	100.3	99	98	97
SiO_2	0.01%	4.87	8.03	7.22	7.32	9.97	21.22	18.04

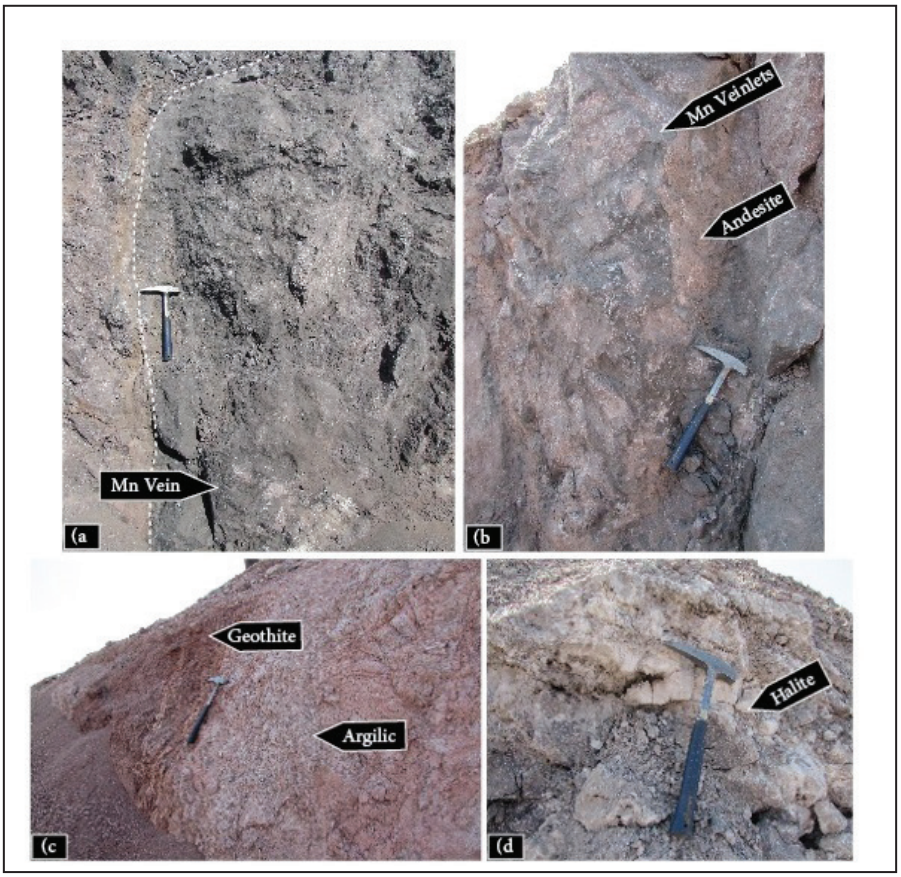

Fig. 3- a) Vein-form structure of the ore (looking westward); b) vein- and veinlet-form structure of the ore within the andesitic host rocks (looking westward); c) argillic and goethitic alterations in the host rock (looking southward); d) halite layer above the Mn veins (looking westward).

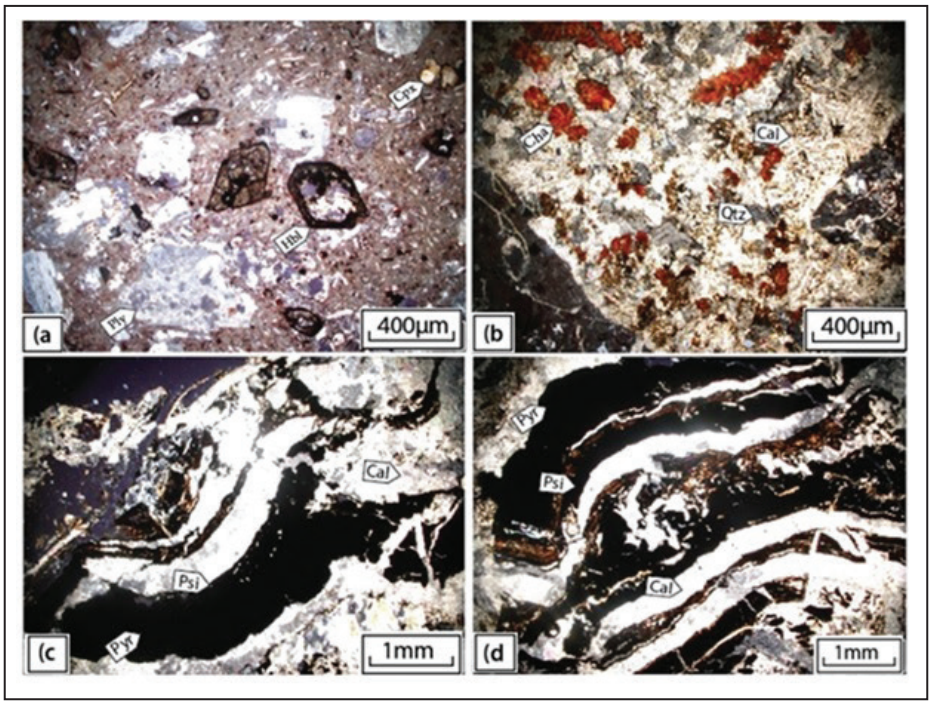

Fig. 4- Microphotographs of: a) porphyritic hornblende andesite (XPL); b) chabazite (red color), carbonate with rhombohedral habit and anhedral grey-color silica (XPL); c and d) colloform texture in Mn ore minerals (XPL, thin section). (Hbl: Hornblende, Cpx: Clino-Pyroxene, Cha: Chabasite, Cal: Calcite, Qtz: Quartz, Psi: Psilomelane, Pyr: Pyrolusite).

The Mn/Fe ratio of the analyzed samples ranges between 2.47 and 113.38, with an average of 48.55, which signifies the differentiation and enrichment of Mn during hydrothermal processes. The average grade of Mn within the veins is estimated about 38.61%

7- 2. Si/Al ratio

The Si/Al ratio is a simple tool to discriminate the hydrothermal, hydrogenous and detrital Mn deposits and to identify their source (Crerar et al., 1982; Bonatti, 1975; Nicholson, 1992). Hydrothermal Mn deposits are generally formed in association with ferrigenous silicic gels and therefore, the Si/Al ratio is high in these deposits. However, Al dominates to Si in deposits of detrital deposits, which is resulted from the decomposition of feldspars during their transport into the sedimentary basin. Holtstam and Mansfeld (2001) believes that if hydrothermal deposits are mixed with clastic fragments (clay minerals), the Si/Al ratio may decrease. The average Si/Al ratio is about 3.14 in the ore samples of Jonub-E Sechangi, falling within the range of hydrothermal deposits (Fig. 5).

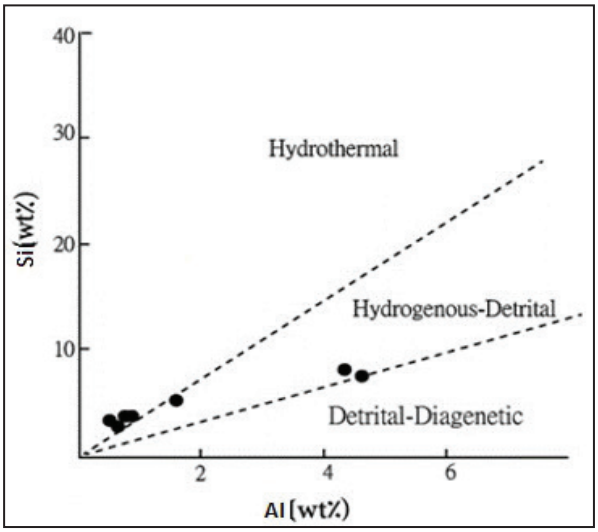

Fig. 5- Si-Al binary diagram (Choi and Hariya, 1992) and the location of the analysed ore samples from the Jonub-e-Sehchangi deposit.

7- 3. (Co+Ni)-(As+Cu+Mo+Pb+V+Zn) binary diagram

This diagram was first used by Nicholson (1992) for discriminating hydrothermal, sedimentary-marine and fresh water deposits. He referred to the enrichment of Sb, Pb, Mo, Li, Cu, Ba, As, Zn, V and Sr as an indicator for hydrothermal deposits, stating that such deposits are also depleted of Ni and Co. Based on the (Fig. 6) diagram, ore samples of the studied Mn veins are enriched in Cu, As, Mo, Zn and Pb, while they are depleted of Ni and Co, testifying to a hydrothermal origin.

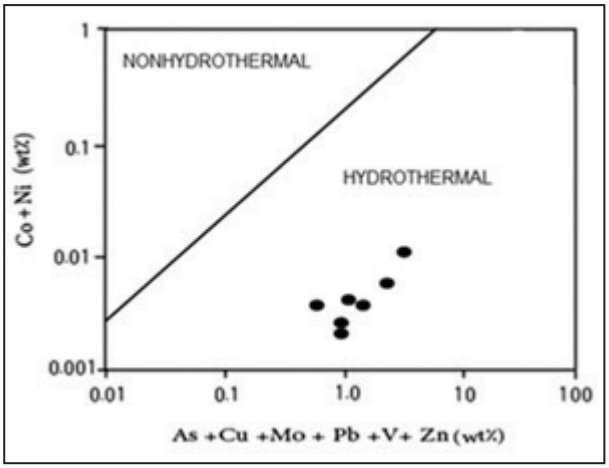

Fig. 6- (Co+Ni)-(As+Cu+Mo+Pb+V+Zn) binary diagram, showing a hydrothermal origin for the Jonub-e-Sehchangi ore samples (Nicholson, 1992).

7- 4. U-Th binary diagram

This diagram was first introduced by Flohrand Huebner (1992) content of the Mn ores is attributed to the clastic particles and is not affected by geochemical processes in oceanic environments (Maynard, 2010). On the other hand, due to the low solubility and very short residence time of Th, this element is not present in the sea water, while hydrothermal activities lead to the concentration and enrichment of U (Heshmat Behzadi and Shahabpour, 2011). Based on this diagram, the studied samples lie within the hydrothermal field (Fig. 7).

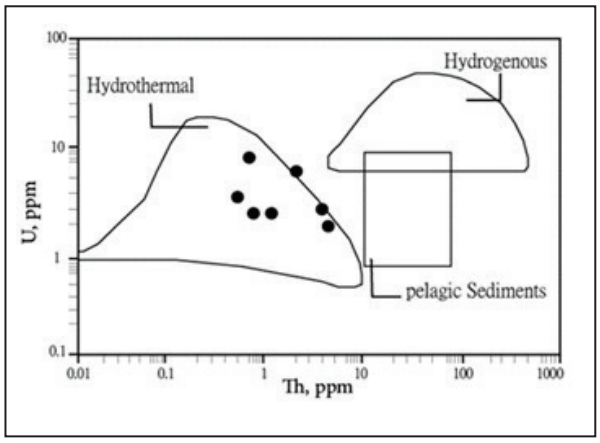

Fig. 7- U-Th binary diagram and the location of the Jonub-e-Sehchangi data points within the hydrothermal field (Bonatti et al., 1976).

7- 5. Fe-Mn-(Ni+Co+Cu)×10 ternary diagram

Many researchers have tried to discriminate Fe-Mn hydrothermal deposits from sedimentary-marine deposits using major and trace elements. Bonatti (1975) proposed the initial Fe-Mn-(Ni+Co+Cu)×10 diagram. According to this diagram, hydrothermal oxides are depleted in Cu,

Co, Ni and Zn compared to sedimentary marine deposits, which can be resulted from their slow rate of precipitation and hence, the longer period of contact with the sea waters and the effect of various processes responsible for the adsorption of these elements (Toth, 1980; Usui and Someya, 1997). Cobalt is intensively adsorbed by Mn oxides and its mean concentration decreases in hydrothermal deposits (Sabation et al., 2001). According to (Fig. 8), the analysed samples fall within the hydrothermal field.

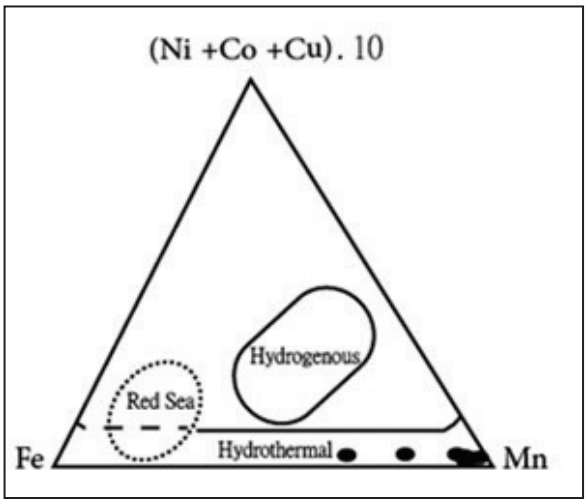

Fig. 8- Fe-Mn-(Ni+Co+Cu)×10 ternary diagram (Bonatti, 1975; Toth, 1980) and the hydrothermal origin determined by it for the Jonub-e-Sehchangi ore deposit.

8- Relationship between major and trace elements

The negative correlation between Al and Mn, as well as Ti-Mn is resulted from different geochemical behavior of these two elements compared with Mn. Manganese is an active element with hydrothermal origin, while Ti and Al are inactive elements with detrital origin (clay minerals), hardly being transported by fluids (Acharya et al., 1997). The positive correlation between Mn and Ba in the studied vein samples indicates their similar geochemical behavior and a common hydrothermal source for them (Holtstam and Mansfeld, 2001). Mn displays the highest positive correlation with Ba, Sr and U and the highest negative relationship with Al, Ti, Mg and Fe, indicating precipitation from a hydrothermal source (Karakus et al., 2010) (Fig. 9).

9- Conclusion

Mn veins of Jonub -E Sehchangi are hosted by volcanic (hornblende andesitic) rocks. Based on mineralographic studies and XRD data, the main Mn minerals are pyrolusite, cryptomelane, psilomelane and hollandite, accompanied by hematite and goethite. Vein-type structure, as well as colloform and open-space filling textures of the ores are indicators of a hydrothermal origin. Based on geochemical studies, the average grade of Mn is about 38.61%, and the average of Mn/Fe ratio is about 48.55 These values, along with the data points plotted in the Si/Al and U/Th diagrams attest to the dominance of hydrothermal processes. Therefore, based on geologic and geochemical evidences, Mn veins in Jonub -E Sehchangi are formed epigenetically through hydrothermal processes. The main source of Mn seems to be the hornblende andesitic rocks of the area. Mn transported by hydrothermal fluids has primarily precipitated as fine-grained Mn^{4+}-oxide-hydroxides, such as cryptomelane, which was later converted to Ba^{2+} and K^{+}rich oxides-hydroxides like psilomelane and hollandite and gradually gave rise to pyrolusite. Considering the extent of volcanic rocks and the occurrence of multiple Mn mineralizations in the Lut Block, this deposit can serve as a model for exploring new reserves.

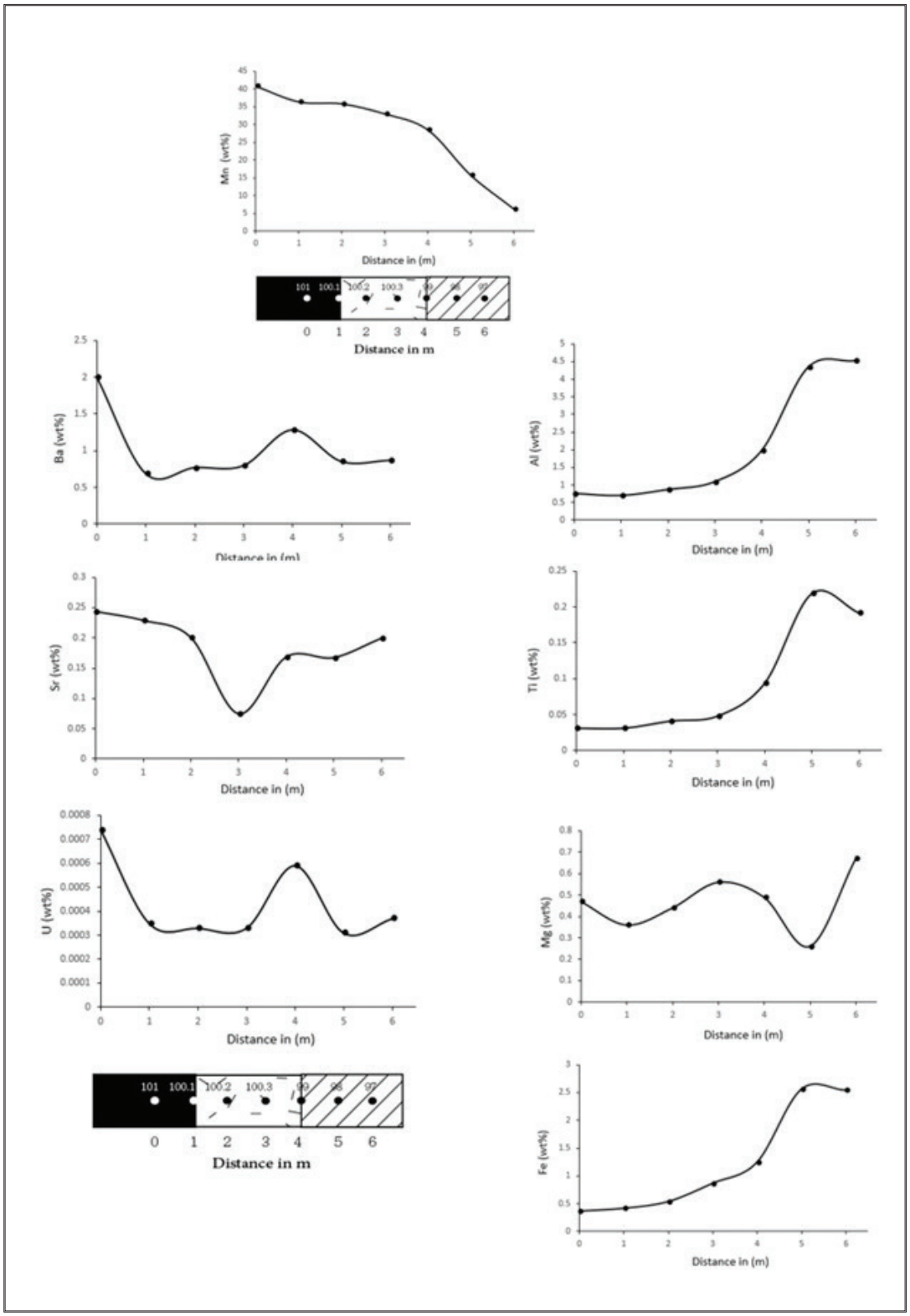

Fig. 9- Distribution diagrams of Mn, Ba, Sr, U, Al, Ti, Mg and Fe from the center towards the wall-rock of the Mn vein.

Acknowledgement

The authors would like to acknowledge the financial support provided by Research Deputy Bureau of the University of Birjand and Tabriz, and the experimental support by Iranian Mineral Processing Research Center (Karaj). Our appreciation is further expressed to anonymous reviewers for making critical comments and suggestions on this manuscript.

References

Acharya, B. C., Rao, D. S. and Sahoo, P. K., 1997- Mineralogy, chemistry and genesis of Nishikhal Manganes ore of south Orissa, India. Miner. Deposita. 32: 79-93.

Aghanabati, A., 1998- Major sedimentary and stuctural units of Iran (map). Geo. sci. J. 7: 29-30.

Arjmandzadeh, R., Karimpour, M. H., Mazaheri, S. A., Santos, S. A. J. F., Medina, J. M. and Homam, S. M., 2011- Sr-Nd isotope geochemistry and petrogenesis of the Chah-Shaljami granitoids (Lut Block, Eastern Iran). J. Asian. Earth. Sci.41: 283-296.

Arjmandzadeh, R. and Santos, J. F., 2014- Sr–Nd isotope geochemistry and tectonomagmatic setting of the Dehsalm Cu–Mo porphyry mineralizing intrusives from Lut Block, eastern Iran. Int. J. Earth. Sci. (Geologische Rundschau) 103: 123–140.

Berberian, M., Jackson, J. A., Qorashi, M., Khatib, M. M., Priestley, K., Talebien, M., Ghafuri Ashtiani, M., 1999- The 1997 May 10 Zirkuh (Qaenat) earthquake (M.W7.2): Faulting along the Sistan suture zone of eastern Iran. Geophys. J. Int. 136: 671–694.

Bolourian, G. H., Vahedi, A., Zohrab, E., Haddadan, M., 2004- Geological map of Iran, Scale 1/100000 Geological Survey of Iran, Tehran.

Bonatti, E., 1975- Metallogenesis at oceanic spreading centers. Annu. Rev. Earth. Pl. Sc. 3: 401-431.

Bonatti, E., Zerbi, M., KAY, R. and Rydell, H., 1976- Metalliferous deposits from the Apennine ophiolites:Mesozoic equivalent of modern deposits from oceanic spreading center: Geol. Soc. Am. Bull. 87: 83-94.

Bonyadi, Z. and Moore, F., 2006- Geochemistry and Genesis of Narigan ferromanganese deposit Bafgh, Yazd province. Sci. Natural 57: 54-63.

Camp, V. E., and Griffis, R. J., 1982- Character, genesis and tectonic setting of igneous rocks in the Sistan suture zone, eastern Iran. Lithos. 15: 221-239.

Choi, J. H. and Hariya, Y., 1992- Geochemistry and depositional environment of Mn oxide deposits in the Tokoro belt, northeastern Hokkaido, Japan. Econ. Geol. 87: 1265–1274.

Crerar, D. A., Namson, J., Chyi, M. S., Willams, L. and Feigenson, M. D., 1982- Manganiferous cherts of the Franciscan assemblage: I. General geology, ancient and modern analogues, and implications for hydrothermal convection at oceanic spreading centers: Eco. Geol. 77: 519-540.

Flohr, M. J. K. and Huebner, J. S., 1992- Mineral assemblages from Sierra Nevada, California ore deposits and proposed origin [abs.]: Geol. Soc. Am. Bull. 20: A300.

Heshmat Behzadi, K. and Shahabpour, J., 2010- Metallogeny of Manganese and Ferromanganese Ores in Baft Ophiolitic Melange, Kerman, Iran. Aust. J. Sci. 4: 302-313.

Holtsatam, D. and Mansfeld, Y., 2001- Origin of carbonate hosted Fe-Mn- (Ba, As, Pb, Sb, W) deposit of Langbon in Central Sweden, Miner. Deposita. 36: 641-657.

Jung, D., Keller, J., Khorasani, R., Marcks, C. H. R., Baumann, A. and Horn, P., 1983- Petrology of the Tertiary magmatic activity the northern Lut area, East of Iran, Ministry of mines and metals. Geological Survey of Iran, Geodynamic Project (Geotraverse) in Iran 51: 285–336.

Karakus, A., Yavuz, B. and Koc, S., 2010- Mineralogy and major trace element geochemistry of the haymana manganese mineralizations, Ankara, Turkey. Geo. Chem. Int. 48: 1014-1027.

Karimpour, M. H. Stern, C. R. Farmer, L. Saadat, S. and Malekezadeh, A., 2011- A Review of age, Rb-Sr geochemistry and petrogenesis of Jurassic to Quaternary igneous rocks in Lut Block, Eastern Iran. J. Petrol. 1: 19-36.

Lotfi, M., 1982- Geological and geochemical investigations on the volcanogenic Cu, Pb, Zn, Sb ore- mineralizations in the Shurab-GaleChah and northwest of Khur (Lut, east of Iran). Unpublished Ph.D thesis, der Naturwissenschaften der Universitat Hamburg, 151 p.

Maynard, J., 2010- The chemistry of manganese: a signal of increasing divercity of earth-surface environments. Eco. Geol. 105: 535-552.

Monazami Bagherzadeh, R., 1994- Genesis of Mn Mineralization in the Darab area (Fars province, Iran). M.Sc. Thesis, University of Shiraz, Shiraz, Iran, 180 pp. (in Persian with English abstract).

Nabatian, G. H., Rastad, E., Neubauer, F., Honarmand, M. and Ghaderi, M., 2015- Iron and Fe–Mnmineralisation in Iran: implications for Tethyan metallogeny, Aust. J. Earth Sci. 62: 211-241.

Nicholson, K., 1992- Contrasting mineralogical-geochemical signatures of manganese oxides: Guides to metallogenesis. Eco. Geol. 87: 1253-1264.

Pang, K. N., Chung, S. L., Zarrinkoub, M. H., Khatib, M. M., Mohammadi, S. S., Chiu, H. Y., Chu, CH. H., Lee, H. Y. and Lo, CH. H., 2013- Eocene-Oligocene post-collisional magmatism in the Lut-Sistan region, eastern Iran: Magma genesis and tectonic implications. Lithos. 180: 234-251.

Richards, J. P., Spell, T., Rameh, E., Razique, A. and Fletcher, T., 2012- High Sr/Y magmas reflect arc maturity, high magmatic water content, and porphyry Cu ± Mo ± Au potential: examples from the Tethyan arcs of central and eastern Iran and western Pakistan. Econ. Geol. 107: 295–332.

Saadat, S., Stern, C. R. and Karimpour, M. H., 2008- Geochemistry of Quaternary Olivine Basalts from the Lut Block, Eastern Iran. American Geophysical Union, Fall Meeting 2008, abstract #T21A-1933.

Saadat, S., Stern, C. R. and Karimpour, M. H., 2009- Quaternary mafic volcanic rocks along the Nayband fault, lut block, eastern iran. Geological Society of America Annual Meeting 18-21 October.

Simmonds, V. and Malek Ghasemi, F., 2007- Investigation of manganese Mineralization in Idahlu and Jokandy, Southwest of Hashtrood, NW Iran. 263-267.

Taghizadeh, S., Mousivand, F. and Ghasemi, H., 2012- Zakeri Mn deposit, example of exhalative mineralization in the southwest Sabzevar31th Symposium on Geosciences, Geological Survey of Iran, Tehran, Iran. (in Persian)

Tarkian, M., Lotfi, M. and Baumann, A., 1983- Tectonic, magmatism and the formation of mineral deposits in the central Lut, east Iran, Ministry of mines and metals. Geological survey of Iran, Geodynamic Project (Geotraverse) in Iran 51: 357-383. Geological Survey of Iran. Tehran, Iran. (in Persian).

Tirrul, R., Bell, l. R., Griffis, J. R. and Camp, V. E., 1983- The sistan suture zone of eastern Iran Geol. Soc. Am. Bull. 94: 134-150.

Toth, J. R., 1980- Deposition of submarine crusts rich in manganese and iron. Geol. Soc. Am. Bull. 91: 44-54.

Usui, A. and Someya, M., 1997- Distribution and composition of marine hydrogenetic and hydrothermal manganese deposits in the northwest Pacific. In: Nicholson, K., Hein, J,R., Bohn, B., Dasgupta, S., (Eds), Manganese Mineralization: Geochemistry and mineralogy of terrestrial and marine Deposits, Geol. Soc. 119: 117-198.

Walker, R. T., Gans, P., Allen, M. B., Jackson, J., Khatib, M., Marsh, N. and Zarrinkoub, M., 2009- Late Cenozoic volcanism and rates of active faulting in eastern Iran. Geophys. J. Int. 177:783- 805.

Zarasvandi, A., Lentz, D., Rezaei, M. and Pourkaseb, H., 2013- Genesis of the Nasirabad manganese occurrence, Fars province, Iran: Geochemical evidences. Chemie. Der. Erde. 73: 495–508.